

# Improvement of sand activation depth prediction under conditions of oblique wave breaking

Xavier Bertin · Bruno Castelle · Giorgio Anfuso · Óscar Ferreira

Received: 29 November 2006 / Accepted: 22 July 2007 / Published online: 14 August 2007  
© Springer-Verlag 2007

**Abstract** This study presents sand activation depth (SAD) measurements recently obtained on two contrasting beaches located along the Atlantic coast of France: the gently sloping, high-energy St Trojan beach where wave incidence is usually weak, and the steep, low-energy Arçay Sandspit beach where waves break at highly oblique angles. Comparisons between field measurements and predictions from existing formulae show good agreement for St Trojan beach but underestimate the SAD on the Arçay Sandspit beach by 40–60%. Such differences suggest a strong

influence of wave obliquity on SAD. To verify this hypothesis, the relative influence of wave parameters was investigated by means of numerical modelling. A quasi-linear increase of SAD with wave height was confirmed for shore-normal and slightly oblique wave conditions, and a quasi-linear increase in SAD with wave obliquity was also revealed. Combining the numerical results with previously published relations, both a new semi-empirical and an empirical formula for the prediction of SAD were developed which showed good SAD predictions under conditions of oblique wave breaking. The new empirical formula for the prediction of SAD ( $Z_0$ ) takes into account the significant wave height ( $H_s$ ), the beach face slope ( $\beta$ ) and the wave angle at breaking ( $\alpha$ ), and is of the form  $Z_0 = 1.6 \tan(\beta) H_s^{0.5} \sqrt{1 + \sin(2\alpha)}$ . The use of a dataset from the literature demonstrates the predictive skill of these new formulae for a wide range of wave heights, wave incidence and beach gradients.

---

X. Bertin (✉)  
Estuaries and Coastal Zones Division,  
National Civil Engineering Laboratory,  
Av. do Brasil 101,  
1700-066 Lisbon, Portugal  
e-mail: xbertin@lnec.pt

B. Castelle  
Griffith Centre for Coastal Management, Griffith University,  
Gold Coast, Queensland 9726, Australia

G. Anfuso  
Departamento de Geología, Facultad de Ciencias del Mar y  
Ambientales, Universidad de Cádiz,  
Polígono Río San Pedro s/n,  
11510 Puerto Real, Cádiz, Spain

Ó. Ferreira  
FCMA/CIMA, Universidade do Algarve,  
Campus de Gambelas,  
8005-139 Faro, Portugal

*Present address:*  
B. Castelle  
UMR CNRS EPOC, Université Bordeaux 1,  
Avenue des Facultés,  
33405 Talence cedex, France

## Introduction

The sediment activation depth (SAD) corresponds to the thickness of the mobile sediment layer at the bed where sediment reworking takes place over an immobile bed (Sherman et al. 1993). Sediment activation depth, often referred to as the disturbance or mixing depth, can be calculated for different time spans ranging from minutes to hours (Kraus 1985; Sunamura and Kraus 1985), to individual tidal cycles (King 1951; Williams 1971; Ciavola et al. 1997; Anfuso et al. 2000) or several days (Greenwood and Hale 1980; Nicholls and Orlando 1993). Irrespective of the time intervals, sediment motion is always caused by

waves, currents, or a combination of both waves and currents (Sunamura and Kraus 1985; Sherman et al. 1993; Ciavola et al. 1997). The ability to accurately predict SAD is of critical importance for the determination of sediment transport in general (Kraus et al. 1982; Kraus 1985; Ciavola et al. 1997; Anfuso 2005) but also for the prediction of potential bed scouring around coastal structures (Fucella and Dolan 1996), the burial or dispersal of contaminants such as oil spills, or for incorporation in models determining the erosion of soft rock shores (Walkden and Hall 2005).

To improve the prediction of SAD, several investigations have been conducted worldwide during the three last decades, mostly based on measuring SAD in different hydrodynamic and beach settings using different methodologies. The oldest method consists of inserting stained natural beach sand into foreshore sediments during low tide (King 1951; Williams 1971; Anfuso et al. 2000). During the following low tide, the mixing depth can be determined by combining measurements of topography and the thickness of the new sand deposited over the plug of stained sand (see Ferreira et al. 2000). Thin steel rods are commonly used to localize the plugs of stained sand and to survey micro-topographic beach changes. Other authors (Greenwood and Hale 1980; Sherman et al. 1993; Anfuso 2005) have inserted rods with loosely fitting washers along foreshore or nearshore profiles. In the course of sediment reworking, the washers move down to the depth of maximum erosion, and the new sediment layer subsequently deposited over the washers constitutes the mixing depth. Finally, another fairly common method consists of the injection of fluorescent tracers into foreshore or nearshore sediments (King 1951; Komar and Inman 1970; Williams 1971; Kraus 1985; Ciavola et al. 1997; Anfuso et al. 2000; Ferreira et al. 2000). After set time intervals, the spatial dispersion of the tracer and the mixing depth are measured by extracting short cores in a closely spaced grid around the injection point, and determining tracer concentrations in a specified number of depth intervals.

Several empirical relations for SAD prediction have been suggested by combining SAD measurements with hydrodynamic data. In this way, it was shown that SAD was a growing function of significant wave height (Williams 1971; Kraus et al. 1982; Kraus 1985; Ciavola et al. 1997; Ferreira et al. 2000; Anfuso 2005). However, the wide scatter of SAD predictions obtained from the different equations suggested that parameters other than significant wave height were involved in controlling SAD. Thus, Sunamura and Kraus (1985) investigated the problem with a more physically based approach, and found a relation between the bed shear stress and SAD. They confirmed that SAD increased approximately linearly with wave height but that it was also slightly dependant on grain size and the wave period of waves higher than 1.5–2 m. Observing

striking SAD differences between steep and gently sloping beaches, Ferreira et al. (2000) proposed a refinement of such relations by including the beach gradient into their prediction formula, thereby considerably improving the accuracy of the predictions. Anfuso et al. (2000) also observed an increase of SAD with the beach gradient when investigating beaches located in SW Spain. They obtained SAD values corresponding to 4 and 16% of breaking wave height for dissipative (slope of 0.02) and intermediate beaches (slope of 0.06) respectively.

However, none of these physical and empirical studies have investigated the influence of wave incidence angle at the breaking point on SAD in any detail. One reason may have been the difficulty in measuring wave directions with sufficient accuracy, because wave incidence angles are often very small, such that the wave angle at breaking is smaller than the error margin. However, since part of the bed shear stress is due to wave-induced longshore currents directly controlled by wave incidence, the influence of wave angle on SAD should be worth investigating.

The main purpose of this study was to investigate the influence of wave obliquity on SAD. To achieve this, SAD measurements were carried out on two contrasting beaches located along the Atlantic coast of France. Among the other measured parameters were significant wave height, wave incidence, and wave period. The influence of these parameters on SAD was then investigated by means of numerical modelling. The different findings were then combined to develop new relations for SAD predictions.

## Study areas

This study combines published data with recently acquired field data obtained on two contrasting beaches located along the middle of the French Atlantic coast, these being the exposed St Trojan beach situated on the open coast in the south of Oléron Island, and a more protected beach along the Arçay Sandspit which is situated in the outer Bertuis-Breton Estuary in the shelter of Ré Island (Fig. 1).

The tides in this region range from less than 2 to more than 6 m, and locally induce tidal currents exceeding  $2 \text{ m s}^{-1}$  (Bertin et al. 2005). At the two study sites, the tidal influence is restricted to water-level variations, and the beaches can thus be classified as wave-dominated. The offshore wave climate is dominated by waves with significant wave heights ( $H_s$ ) ranging from 1 to 2 m, peak periods of 8–12 s, and W–NW directions. In winter, North Atlantic low-pressure systems can generate westerly swells with  $H_s$  exceeding 4 m, which occur more than 5% of the time (Bertin 2005; Bertin et al. 2007).

The St Trojan beach (Fig. 1b) is composed of fine sand ( $D_{50}=0.18\text{--}0.22 \text{ mm}$ ) which, together with the energetic

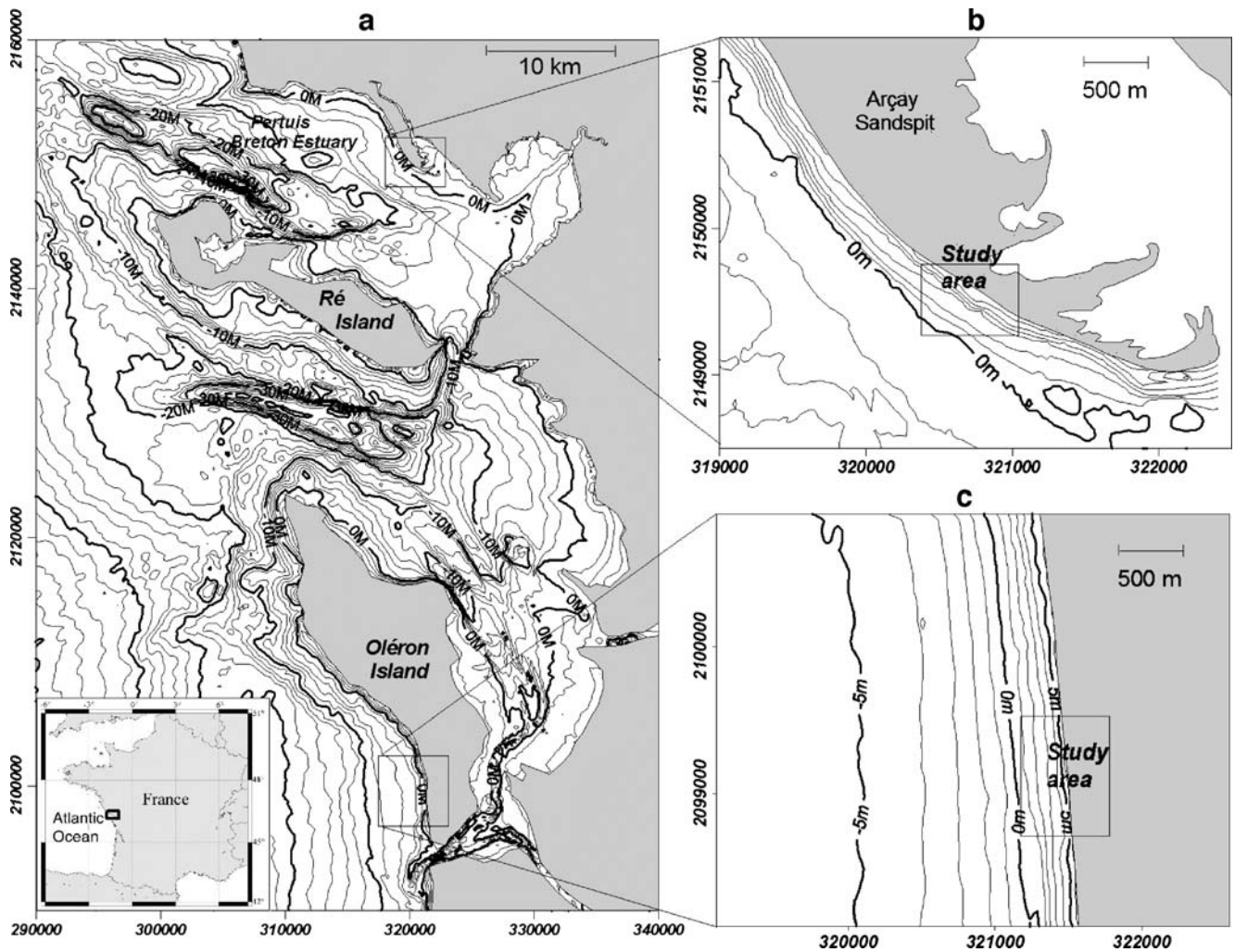


Fig. 1 General location (a), and detailed bathymetric maps of the Arçay Sandspit beach (b) and the St Trojan beach (c)

wave climate, causes its morphology to be dissipative for most of the time, according to the classification of Masselink and Short (1993). The shoreface has a concave shape, and the beach gradient is nearly constant within the intertidal zone ( $\tan\beta=0.015$ ). Given the gently sloping and shallow shoreface, wave incidence at breaking is greatly reduced and lies mostly in the range of 0–5° (Bertin 2005).

The beach along the Arçay Sandspit (Fig. 1c), by contrast, is more sheltered, and wave-energy attenuation decreases wave heights by more than 70% relative to offshore conditions (Bertin et al. 2007). The beach displays a low-tide terrace with a gently sloping, lower section consisting of fine sands ( $\tan\beta=0.015$  and  $D_{50}=0.2$  mm), and a steep upper section consisting of coarse sands ( $\tan\beta=0.06$  and  $D_{50}=0.6$  mm). Given a shoreline orientation of 215°N and swells originating from the W–NW, the waves can break with incidence angles of up to 30° at high tide (Bertin et al. 2007).

**Materials and methods**

**Topographic and bathymetric surveys**

The beach morphologies were surveyed by using a combination of hydrographic depth surveys at high tide and overlapping topographic surveys at low tide, the latter also being used to check the reliability of the bathymetric measurements. The St Trojan beach was surveyed on 4 April 2006 using a Septentrio® Polar X2 Real Time Kinematic GPS, the mobile antenna of which was mounted on a bicycle. The accuracy of this GPS is about 1 cm in the horizontal and 2 cm in the vertical direction. The shoreface of the beach was surveyed on 1 April 2006 at high tide by the local hydrographic office (Direction Départementale de l’Equipement 17).

The Arçay Sandspit beach was surveyed on 27 April 2006 from a four-wheel-drive vehicle equipped with the

same GPS as that used for the St Trojan surveys. This was complemented on 30 May 2006 by a bathymetric survey using a Navysound 215 bi-frequency (38–200 Hz) echosounder and the same GPS as that for the topography.

The original position data, acquired in WGS 84 format, were converted into Lambert II planar and metric coordinates, this being the working coordinate system used throughout the study.

#### Sand activation depth (SAD)

In each of the two study areas, SAD was determined by two different methods, enabling a critical comparison of results and a reliability check of these methods. Following the methodology widely adopted in previous studies (Ingle 1966; Komar and Inman 1970; Ciavola et al. 1997; Ferreira et al. 2000), plug holes 20–40 mm in diameter were filled with fluorescent tracers (*method 1*). The tracers were emplaced at low tide, and each hole was positioned by using the GPS described above. SAD was measured during the following low tide, by assessing the change in tracer thickness within each hole, thereby avoiding the need for micro-topographic measurements. In any case, a comparison of SADs obtained in this manner and the thickness of tracer replaced by natural sand did not show statistically significant differences.

At the same time, fluorescent tracer experiments were conducted in each study area, and additional SAD measurements were made using short cores extracted at the centres of the fluorescent tracer clouds (*method 2*). These cores were cut lengthwise, and analysed under a UV lamp in the laboratory. Following Komar and Inman (1970), SAD was in this case defined as the maximum depth of tracer burial. This definition was given preference to the 80% cut-off rate proposed by Kraus et al. (1982) because, at least on the St Trojan beach, tracer concentration was always very low.

In both study areas, SAD values obtained by the two methods differed by less than 10–20% for a given position along each beach profile. The average value for each position along the beach profile was then used for further analyses, although the entire range of values is presented here.

For the St Trojan beach, SAD measurements took place on 1 and 4 April 2005, and on 6 and 28–29 April 2006 during concomitant tracer experiments aimed at determining the longshore transport on this beach (Bertin et al., unpublished data). During each experiment, three to four SAD measurements were done according to method 1, in the vicinity of the main tracer injection point located 0.5–1 m below mean sea level (Fig. 2). During the measurements, the water level changed by more than 4 m in the course of the tidal cycle. The tracer zone thus experienced about 7 h of wave action, which alternatively consisted of wave swash, wave breaking and wave shoaling. Nine to ten

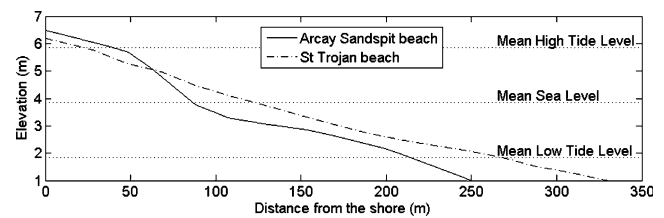


**Fig. 2** Cross-shore profiles of the study beaches at the location of SAD measurements

additional cores were collected for method 2 during each of the four surveys.

For the Arçay Sandspit beach, the first experiment (11 April 2006) consisted of six tracer plug holes placed along a cross-shore profile (method 1). Since this experiment revealed a 300% increase in SAD from the lower beach to the upper beach, it was decided to divide the beach into three zones for the two following experiments (13 and 26 April 2006): (1) the lower beach, corresponding to the low-tide terrace around 2–3 m above the lowest astronomical tide (LAT; Fig. 2); (2) the middle beach, corresponding to the transition between the low-tide terrace and the steep upper beach (around mean sea level; Fig. 2); and (3) the upper beach, corresponding to the steep part around 4–5 m above LAT (Fig. 2). A different tracer colour was used at each injection point, and SAD measurements based on method 1 were done in the middle of each of the three beach zones. The consistency of SAD for a given position along the beach profile was also checked from the analysis of the sliced cores sampled for method 2 during each of the two tracer experiments on 13 and 26 April 2006 (73 and 78 cores respectively).

#### Hydrodynamics

Wave and wave-induced currents were recorded using a S4-ADW (InterOcean®) current meter, deployed on the lower beach at St Trojan beach and in the middle of the intertidal zone at the Arçay beach.

Sea surface elevations were estimated assuming that the pressure field was hydrostatic, as demonstrated by Lin and Liu (1998). Data processing was then performed by subdividing the entire record into consecutive time sections of 240 s.

Power spectral estimates  $S(f)$  were computed by 75% overlapping Fourier transforms, Hanning windowed. The significant wave height  $H_s$  (m) was defined as four times the square root of the zero moment  $m_0$  of the wave power spectrum  $S(f)$ , and the peak period was determined as the inverse of the frequency at which the maximum energy was found.

The peak wave direction  $\text{Dir}_p$  ( $^\circ$ ) was computed from the free surface elevation ( $\xi$ ) and the horizontal velocity

components ( $u$  and  $v$ ), using cross spectra  $C_{xy}(f)$  according to Eq. 1:

$$\text{Dir}_p = \arctan\left(\frac{a}{b}\right) \quad (1)$$

where

$$a = \max [C\xi u(f)] \quad (2)$$

and

$$ab = \max [C\xi v(f)] \quad (3)$$

Numerical modelling of bed shear stress

### Model description

The time- and depth-averaged coastal area model MORPHODYN (Saint-Cast 2002), driven by the spectral wave model SWAN (Booij et al. 1999), was used in the present study. This model has previously been successfully applied to simulate wave-induced currents over an alongshore-uniform multiple-barred beach (Castelle et al. 2006a), and to generate both crescentic bar patterns and transverse bar and rip morphologies (Castelle et al. 2006b) as well as to estimate both longshore current magnitude and longshore transport rates along the St Trojan beach (Bertin 2005).

Due to the almost alongshore-uniform configuration of St Trojan beach, it was decided to use the 1DH mode of this numerical model. Wave outputs were extracted from a 10-m resolution grid along the cross-shore profile crossing the S4 current-meter location, and extending from the dune to approximately 20 m below LAT on the St Trojan beach.

Bed shear stress was parameterised as being proportional to mean flow by means of a bottom friction coefficient  $C_f$  and the wave orbital velocity near the bottom  $U_w$ , following the weak flow approximation of Liu and Dalrymple (1978):

$$\tau = \rho C_f U_w U_c \quad (4)$$

where  $\rho$  is the mass density of seawater,  $U_c$  the wave-induced current magnitude, and  $C_f$  a spatially constant bottom friction coefficient. Bottom friction calibration of both Castelle et al. (2006a) and Bertin et al. (unpublished data) showed that best agreements with field data were obtained for  $C_f=0.0048$ .

### Modelling strategy

The model was run in stationary mode, using a constant sea level corresponding to mean sea level. As the SAD measurements described above took place in a macrotidal environment, any area located on the lower beach experienced several wave processes (swash, breaking, shoaling)

and, thus, several bed stress events during a tidal cycle. Nevertheless, the SAD recorded during the subsequent low tide was considered to result from the maximum stress at the bed during the tidal cycle. Consequently, during each numerical simulation, the maximum computed bed shear stress ( $\tau$ ) along the beach profile was extracted to document the relative influence of wave parameters on both bed shear stress and SAD.

The first step of the numerical computations consisted of running the model with boundary conditions corresponding to wave conditions prevailing during the four SAD measurement campaigns conducted at St Trojan beach. This was done in order to investigate the relation between bottom shear stress ( $\tau$ ) and SAD.

The second step consisted of tuning the offshore boundary conditions in order to fix two of the wave parameters at the breaking point (e.g. wave period and wave incidence angle), whereas the third one (e.g.  $H_s$ ) varied from one simulation to another. Relatively restricted ranges for wave parameters were tested ( $0 < H_s < 1.5$  m;  $0 < \text{Dir} < 9^\circ$ ;  $7 < T_p < 13$  s), in order to comply with the approximation of Liu and Dalrymple (1978) stating that steady currents must be weak relative to wave orbital currents.

## Results

### Sand activation depth

For the St Trojan experiments,  $H_s$  at breaking ranged from 0.4 to 2.0 m. Sand activation depth displayed very small spatial variability in all experiments. Average SAD values were very low (Table 1), and ranged from  $0.015 \pm 0.003$  m for low-energy conditions ( $H_s=0.4$  m) to  $0.05 \pm 0.01$  m for high-energy wave conditions ( $H_s=2.0$  m).

Tracer experiments at the Arçay Sandspit enabled measuring SAD for  $H_s$  ranging from 0.2 to 0.6 m. Despite only three experiments being conducted, a wide range of wave incidence angles was covered because, in the period from low to high tide, wave incidence increased by over  $15^\circ$  (Bertin et al. 2007). SAD values showed a marked cross-shore variability, ranging from  $0.015 \pm 0.005$  m on the lower beach for very low wave-energy conditions ( $H_s=0.20$  m) to  $0.11 \pm 0.01$  m on the upper beach for low- to moderate-energy conditions ( $H_s=0.6$  m).

### Relation between SAD and bottom shear stress

The first step of the numerical study was to verify the assumption that SAD is a function of total bed stress. This was done only for the St Trojan beach because an intensive calibration of the model was already available for this beach at that time (Bertin et al., unpublished data). Wave

**Table 1** Wave parameters, beach slope, and measured and predicted sand mixing depth (SAD) on the St Trojan beach and the Arçay Sandspit beach (*n.a.* not available)

Place and date	Significant wave height	Wave period	Wave angle	Beach slope, $\tan\beta$	SAD measured	SAD predicted from Anfuso et al. (2000)	SAD predicted from Ferreira et al. (2000)
	(m)	(s)	(°)	(–)	(m)	(m)	(m)
St Trojan (01/04/2005)	0.4	7	3	0.015	0.015±0.003	0.016	0.011
St Trojan (04/04/2005)	0.9	10.5	4.5	0.015	0.027±0.004	0.036	0.025
St Trojan (06/04/2005)	1.1	11.5	5.5	0.015	0.032±0.006	0.044	0.031
St Trojan (28–29/03/2006)	2.0	10	3	0.015	0.05±0.01	0.080	0.056
Arçay Sandspit (11/04/2006), upper beach	0.6	12	25	0.06	0.11±0.01	0.096	0.067
Arçay Sandspit (13/04/2006), upper beach	0.4	11	30	0.06	0.08±0.01	0.064	0.045
Arçay Sandspit (13/04/2006), middle beach	0.35	11	20	0.015	0.035±0.005	0.014	0.01
Arçay Sandspit (13/04/2006), lower beach	0.25	n.a.	n.a.	0.015	0.015±0.005	0.01	0.007
Arçay Sandspit (23/4/2006), upper beach	0.35	12	25	0.06	0.072±0.015	0.056	0.039
Arçay Sandspit (26/04/2006), middle beach	0.3	12	15	0.015	0.025±0.005	0.012	0.008
Arçay Sandspit (26/04/2006), lower beach	0.2	n.a.	n.a.	0.015	0.015±0.005	0.008	0.006

boundary conditions were tuned offshore in order to reproduce, as closely as possible, the wave parameters recorded by the S4-ADW during each mixing depth experiment. The model results clearly show that SAD is a growing function of total bottom shear stress (Fig. 3), as previously demonstrated by Sunamura and Kraus (1985), and that SAD is well reproduced with the function

$$Z_0 = C_1 \sqrt{\max(0, \tau - \tau_{cr})} \quad (5)$$

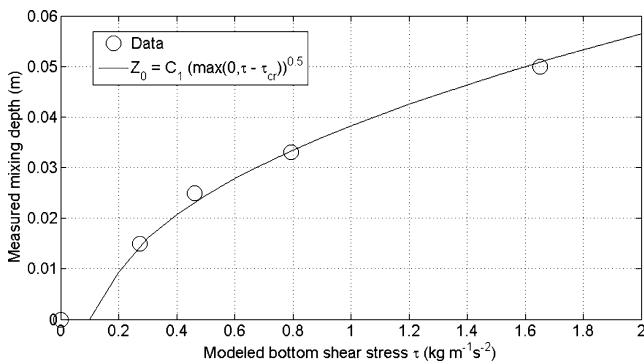


**Fig. 3** Measured sand mixing depth as a function of modelled total bed shear stress and adjustment with a relation of the form  $Z_0 = C_1 \sqrt{\max(0, \tau - \tau_{cr})}$ , where  $C_1$  has been empirically adjusted to a value of 0.041

where  $C_1$  has been empirically adjusted to a value of 0.041, and  $\tau$  is the bed shear stress and  $\tau_{cr}$  a critical bed shear stress below which no movement takes place at the bottom.

#### Influence of wave parameters on bottom shear stress

The second step of the numerical study consisted of testing the relative influence of wave parameters on total bed shear stress. A major advantage of numerical modelling is that it offers the unique opportunity of testing the influence of a given wave parameter, while the others can be kept rigorously constant.

#### Wave height

To test the influence of  $H_s$ , wave parameters were tuned offshore in order to provide constant values for the peak period (10 s) and for the wave angle ( $2^\circ$ ) at the breaking point. The test clearly shows that bed shear stress  $\tau$  is a growing function of wave height at breaking (Fig. 4). Model run results are in good agreement with the relation

$$\tau = C_2 H_s^2 + C_3 H_s \quad (6)$$

where  $C_2$  and  $C_3$  are empirical constants adjusted to 0.85 and 0.15 respectively.

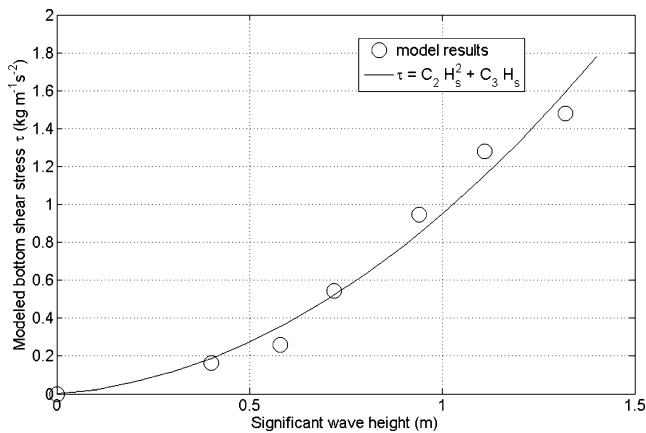


**Fig. 4** Modelled total bed shear stress as a function of wave height and adjustment with a relation of the form  $\tau = C_2H_s^2 + C_3H_s$ , where  $C_2$  and  $C_3$  have been empirically adjusted to 0.85 and 0.15 respectively

*Wave angle at breaking*

The influence of wave angle at breaking ( $\alpha$ ) was tested by tuning offshore wave conditions in order to provide constant wave periods (10 s) and wave height (1.15 m), but variable wave incidences at the breaking point. Model results show a close to linear positive relation between wave incidence at breaking and total bottom shear stress (Fig. 5). These data suggest a non-zero value for frontal waves ( $\alpha=0^\circ$ ), which should correspond to the component of the bottom shear stress due to wave orbital motions  $\tau_0$ . Model results can be adjusted by the function

$$\tau = \tau_0 + C_4 \sin(2\alpha) \tag{7}$$

where  $C_4$  has been empirically adjusted to a value of 5.5 and  $\tau_0$  to 0.85.

*Wave period*

Testing the effect of peak wave period was the most critical aspect, because wave period controls wave height and wave incidence at the breaking point. Offshore wave parameters were thus carefully tuned to obtain variable peak periods,

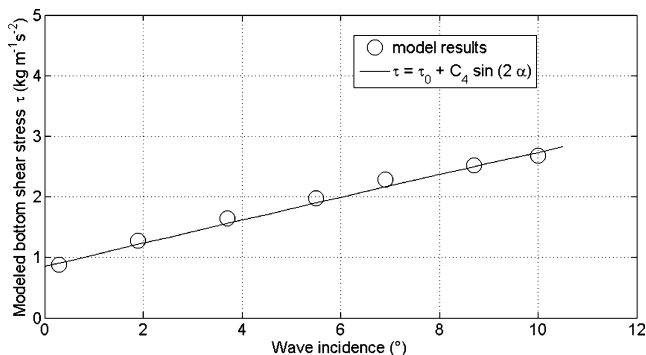


**Fig. 5** Modelled total bed shear stress as a function of wave incidence at breaking and adjustment to a relation of the form  $\tau = \tau_0 + C_4 \sin(2\alpha)$ , where  $C_4$  has been empirically adjusted to a value of 5.5 and  $\tau_0$  to 0.85

but constant  $H_s$  (1.15 m) and wave incidence ( $\alpha=4^\circ$ ) at the breaking point. The results show no clear influence of peak wave period on total bottom shear stress (Fig. 6).

**Discussion**

*Sand activation depth*

Comparing our data from the St Trojan beach with the predictions derived from the relation of Ferreira et al. (2000), an overall good agreement is evident (Table 1). Field measurements were also compared with the predictions derived from the relation proposed by Anfuso et al. (2000), who suggested that SADs correspond to 4% of the breaking wave height for dissipative beaches. This relation thus clearly overestimates the SADs measured on the St Trojan beach (Table 1).

On the Arçay Sandspit beach, predictions from the relation of Ferreira et al. (2000) systematically underestimate the measured values by 40–60% (Table 1). The comparison with predictions from Anfuso et al. (2000), who suggested SAD to be equal to 16% of  $H_s$  for intermediate beaches (the steeper part of the beach) and 4% for dissipative beaches (the low-tide terrace), also shows 50% underestimations of the SADs recorded on the Arçay Sandspit beach.

The systematic differences between our measured values for oblique wave incidence and those generated by the application of published “predictive” equations prompted us to investigate whether these equations could be improved by including a term for oblique wave incidence (cf. below). On the contrary, the lack of any clear correlation between peak wave period and bed shear stress in our study confirms the results of Sunamura and Kraus (1985), who found no evident relation with the peak period for waves with  $H_s < 1.5$  m. Nevertheless, these authors reported that SAD could be a function of wave period for larger breaking waves. This hypothesis was not tested in

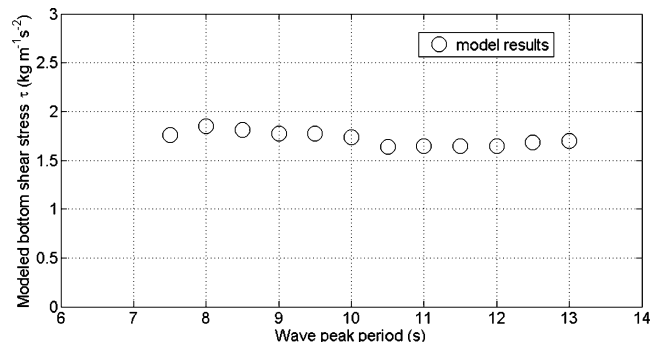


**Fig. 6** Modelled total bed shear stress as a function of peak wave period

our numerical study because, for large waves, the approximation of Liu and Dalrymple (1978) can not be applied.

#### New method for SAD prediction

Our numerical simulations have shown that SAD ( $Z_0$ ) is a growing function of the total bed shear stress  $\tau$ . This is in agreement with the findings of Sunamura and Kraus (1985). According to Van Rijn (1989), the total bed shear stress  $\tau$  can be written as the sum of the bed shear stress due to wave orbital motions,  $\tau_0$ , and the bed shear stress due to steady wave-induced currents,  $\tau_{st}$ :

$$\tau = \tau_0 + \tau_{st} \quad (8)$$

Combining this with Eq. 5 gives

$$Z_0 = C_1 \sqrt{\max(0, \tau_0 + \tau_{st} - \tau_{cr})} \quad (9)$$

Then, based on the numerical results of the tests on the influence of  $H_s$  and wave incidence (Eqs. 6 and 7), it can be argued that  $\tau_{st}$  has the form

$$\tau_{st} = C_{34} H_s \sin(2\alpha) \quad (10)$$

where  $C_{34}$  is an empirical constant.

In the same manner and considering the work of Van Rijn (1989), the bed shear stress due to steady wave-induced currents  $\tau_0$  is assumed to be of the form

$$\tau_0 = C_5 H_s^2 \quad (11)$$

where  $C_5$  is an empirical constant.

By combining Eqs. 9, 10 and 11, a new relation can be established for the prediction of SAD:

$$Z_0 = C_1 \sqrt{\max(0, C_5 H_s^2 + C_{34} H_s \sin(2\alpha) - \tau_{cr})} \quad (12)$$

Considering the work of Ferreira et al. (2000), which suggests a linear relation between SAD and the beach gradient  $\beta$ , the term  $C_1$  of Eq. 12 can be replaced by  $C_1' \tan\beta$ :

$$Z_0 = C_1' \tan(\beta) H_s^{0.5} \sqrt{\max\left(0, C_5 H_s + C_{34} \sin(2\alpha) - \frac{\tau_{cr}}{H_s}\right)} \quad (13)$$

This equation implies that for shore-normal or slightly oblique wave conditions, the term which accounts for the wave angle at breaking would become negligible, causing the SAD to be a close to linear growing function of the significant wave height. Such a property corroborates the findings of Sunamura and Kraus (1985), and is also in agreement with empirical relations proposed by Anfuso et al. (2000) and Ferreira et al. (2000). On the contrary, under oblique wave conditions, this term would not be negligible

and would cause the SAD to no longer be a linear function of the significant wave height. This important difference of Eq. 13 with previously published relations could explain why these relations are not suitable for predicting SAD under oblique wave conditions.

The reliability of this new relation was tested with all the data found in the literature (Sunamura and Kraus 1985; Ferreira et al. 1998; Anfuso et al. 2000, 2003; Anfuso and Ruiz 2004) where the required parameters were available (Table 2, Fig. 7a). Coefficients  $C_1'$ ,  $C_{34}$  and  $C_5$  were determined empirically, the best predictions being obtained with  $C_1'=1.2$ ,  $C_{34}=4$ ,  $C_5=2.2$  and  $\tau_{cr}=0.05$ . When calibrated with these empirical coefficients, Eq. 13 produces predictions which are in good agreement with the field data tested in this study ( $R^2=0.92$ ). Nevertheless, it could be argued that the semi-empirical Eq. 13 is not easy to apply, particularly in the field. To overcome this problem, a simplified version of Eq. 13 was derived empirically:

$$Z_0 = C_6 \tan(\beta) H_s^{0.5} \sqrt{1 + \sin(2\alpha)} \quad (14)$$

where  $C_6$  is a constant which has been empirically adjusted to a value of 1.6 using the dataset of Table 2. Equation 14 produces predictions for SAD ( $R^2=0.93$ ) within the same order of accuracy as for Eq. 13 when applied to the same dataset (Table 2, Fig. 7b). Due to its simplicity, this simplified empirical relation may be preferred to Eq. 13.

Since the data used for this correlation originate from coastlines around the world and cover a wide range of  $H_s$  ( $0.25 < H_s < 2.0$  m), wave incidence ( $0 < \alpha < 30^\circ$ ) and beach gradient ( $0.015 < \tan\beta < 0.14$ ), these two new equations can claim a broad applicability. Their application produces accurate predictions of SAD, particularly in cases where waves approach the coast at oblique angles, such as at the Arçay Sandspit beach. More generally, they constitute a significant improvement over the relation of Ferreira et al. (2000) which, when applied to the same dataset, resulted in poorer predictions ( $R^2=0.87$ ).

It is emphasised that the empirical constants proposed for Eqs. 13 and 14 have been adjusted using the available dataset from the international literature as well as the field data presented in this study. As Eqs. 13 and 14 were also derived using these new field data, the two new formulae should be worth testing and validating with new and independent datasets.

## Conclusions

This study has demonstrated that the influence of wave angle at breaking cannot be ignored when computing sediment activation depth on the basis of currently available predictive equations. The analysis of our field data from a

**Table 2** Data used to test sand activation depth (SAD) predicted from the new semi-empirical relation developed in this study (Eq. 13) and from the empirical relation derived from it (Eq. 14)

Authors	Place and date	Significant wave height	Wave period	Wave angle	Beach slope, $\tan\beta$	SAD measured	SAD predicted from Eq. 13	SAD predicted from Eq. 14
		(m)	(s)	(°)	(–)	(m)	(m)	(m)
This study	St Trojan (01/04/2005)	0.4	7	3	0.015	0.015	0.013	0.016
	St Trojan (04/04/2005)	0.9	10.5	4.5	0.015	0.027	0.028	0.024
	St Trojan (06/04/2005)	1.1	11.5	5.5	0.015	0.032	0.034	0.027
	St Trojan (28–29/04/2006)	2.0	10	3	0.015	0.05	0.056	0.036
	Arçay Sandspit (11/04/2006)	0.6	12	25	0.06	0.11	0.117	0.099
	Arçay Sandspit (13/04/2006)	0.4	11	30	0.06	0.08	0.095	0.083
	Arçay Sandspit (13/04/2006)	0.35	11	20	0.015	0.035	0.019	0.018
	Arçay Sandspit (26/04/2006)	0.35	12	25	0.06	0.072	0.083	0.075
	Arçay Sandspit (26/04/2006)	0.30	12	15	0.015	0.025	0.016	0.016
	Sunamura and Kraus (1985)	Aijgaura (14/12/1978)	1.00	9	6	0.017	0.038	0.035
Aijgaura (31/03/1979)		1.10	6.5	2	0.017	0.029	0.035	0.03
Oraï (12/08/1980)		1.00	10.2	8	0.015	0.028	0.033	0.027
Oraï (27/08/1981)		1.10	6.1	6	0.015	0.023	0.034	0.028
Oraï (26/08/1982)		0.80	7.5	4	0.020	0.019	0.033	0.031
Ciavola et al. (1997)	Faro (03/07/1996)	0.80	7	20	0.14	0.22	0.249	0.204
	Culatra (10/07/1993)	0.37	5.8	5	0.11	0.106	0.098	0.116
	Culatra (10/07/1993)	0.34	5.1	5	0.11	0.106	0.091	0.111
Anfuso et al. (2000)	Rota (11/09/1996)	0.52	10	7	0.06	0.085	0.075	0.077
	Rota (03/08/1997)	0.58	11	15	0.06	0.075	0.099	0.09
	La Ballena (07/03/1997)	0.35	4.5	2	0.04	0.044	0.029	0.039
	Tres Piedras (01/10/1997)	0.70	10	5.5	0.02	0.030	0.03	0.029
	Tres Piedras (02/10/1997)	0.45	10	5.4	0.02	0.018	0.021	0.023
	Tres Piedras (30/11/1997)	0.80	12	3	0.02	0.040	0.032	0.03
Anfuso et al. (2003)	Aguaduce (30/11/1997)	0.90	12	3	0.05	0.060	0.088	0.08
	La Barossa (03/09/2003)	0.50	9	3	0.02	0.030	0.031	0.036

**Table 2** (continued)

Authors	Place and date	Significant wave height	Wave period	Wave angle	Beach slope, $\tan\beta$	SAD measured	SAD predicted from Eq. 13	SAD predicted from Eq. 14
		(m)	(s)	(°)	(–)	(m)	(m)	(m)
Anfuso and Ruiz (2004)	Faro (13/05/2002)	0.50	4	0	0.02	0.030	0.018	0.023
	Faro (13/05/2002)	0.50	4	2.5	0.11	0.090	0.114	0.131
Ferreira et al. (1998)	Quarteira (27/03/1996)	0.49	12.3	4.6	0.11	0.107	0.12	0.133
	Quarteira (15/03/1997)	0.60	10.65	8.2	0.10	0.160	0.145	0.14
	Quarteira (18/03/1997)	0.81	9.9	4.9	0.10	0.153	0.169	0.156
	Quarteira (20/03/1997)	0.61	9.3	6.7	0.12	0.144	0.169	0.166
	Faro (24/04/1997)	0.85	9.35	10.2	0.14	0.172	0.279	0.24

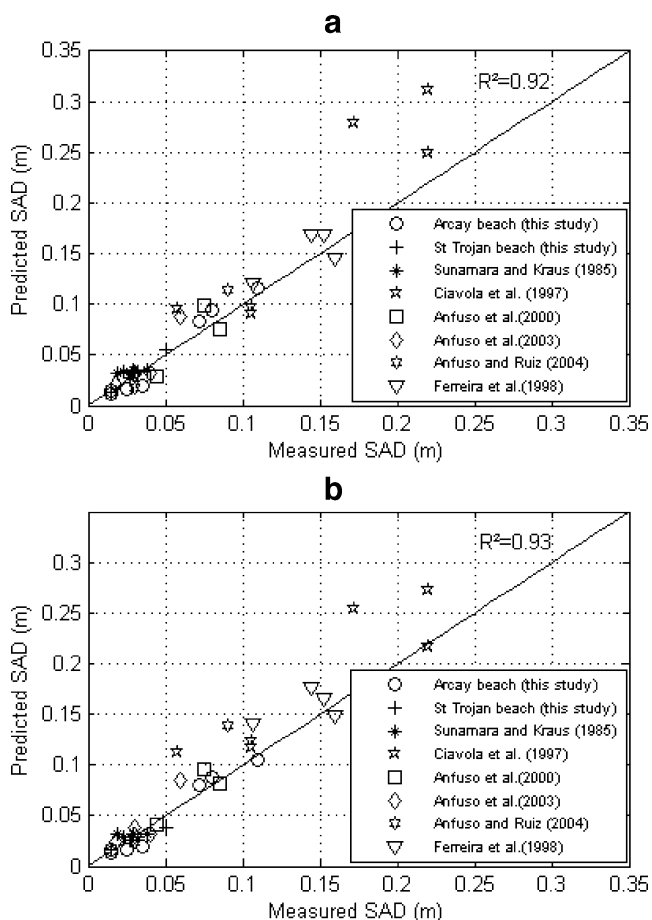


**Fig. 7** Correlation between measured and predicted SADs: **a** based on semi-empirical Eq. 13; **b** based on empirical Eq. 14, as derived from Eq. 13

beach where waves break at angles exceeding  $20^\circ$  shows a strong influence of wave angle at breaking on SAD. Subsequent numerical tests on the relative influence of wave parameters have confirmed

1. a quasi-linear increase in SAD with wave height for shore-normal wave conditions;
2. a close to linear increase in SAD with wave angle; and
3. a lack of clear relationship between SAD and wave period.

Combining these numerical results, a new semi-empirical and a simpler empirical equation which both account for wave angle at breaking were developed, and have enabled us to obtain good SAD predictions over a wide range of wave heights, wave incidence and beach gradients.

It is suggested that the accuracy of the new equations should be further tested, especially for high-energy settings ( $H_s > 1.5\text{--}2$  m) and under conditions of oblique wave incidence. These equations can be used to improve the planning of tracer experiments, and be integrated into numerical models used in sand transport predictions.

**Acknowledgements** The first author is funded by the European Commission through a Marie Curie Intra-European Fellowship (contract IMMATIE MEIF-CT-2006-041171). Eric Chaumillon, Jonathan Allard, Stéphane Recoura, Pascal Tiphaneau, Robin Quique and Antoine Deshouilleres are thanked for their help during fieldwork. Jacques Marquis from the ONCFS has allowed us to work within the Arcay nature reserve. This work is a contribution to the Andalusia PAI Research Group RNM-328. Óscar Ferreira participated under the scope of the BERNIA (POCTI/CTA/45431/2002) project.

## References

- Anfuso G (2005) Sediment activation depth values for gentle and steep beaches. *Mar Geol* 220:101–112
- Anfuso G, Ruiz N (2004) Morphodynamic of a mesotidal, low tide terrace exposed beach (Faro, South Portugal). *Cienc Mar* 30 (4):575–584
- Anfuso G, Gracia FJ, Andrés J, Sánchez F, Del Río L, López F (2000) Depth of disturbance in mesotidal beaches during a single tidal cycle. *J Coast Res* 16(2):446–457
- Anfuso G, Benavente J, Del Río L, Castiglione E, Ventorre M (2003) Sand transport and disturbance depth during a single tidal cycle in a dissipative beach: La Barrosa (SW Spain). In: Sanchez-Arcilla A, Bateman A (eds) Proc 3rd IAHRD Symp River, Coastal and Estuarine Morphodynamics (RCEM 2003), Madrid, Vol 2. IAHRD publication, Madrid, pp 1176–1186
- Bertin X (2005) Morphodynamique séculaire, architecture interne et modélisation d'un système baie/embouchure tidale: le Pertuis de Maumusson et la Baie de Marennes-Oléron. PhD Thesis, La Rochelle University
- Bertin X, Chaumillon E, Sottolichio A, Pedreros R (2005) Tidal inlet response to sediment infilling of the associated bay and possible implications of human activities: the Marennes-Oléron Bay and Maumusson Inlet, France. *Cont Shelf Res* 25:1115–1131
- Bertin X, Deshouillieres A, Allard J, Chaumillon E (2007) A new fluorescent tracers experiment improves understanding of sediment dynamics along the Arçay Sandspit (France). *Geo-Mar Lett* 27(1):63–69
- Booij N, Ris RC, Holthuijsen LH (1999) A third generation wave model for coastal regions. Part I: model description and validation. *J Geophys Res* 104:7649–7666
- Castelle B, Bonneton P, Sénéchal N, Dupuis H, Butel R, Michel D (2006a) Dynamics of wave-induced currents over an alongshore non-uniform multiple-barred sandy beach on the Aquitanian Coast, France. *Cont Shelf Res* 26:113–131
- Castelle B, Bonneton P, Butel R (2006b) Modeling of crescentic pattern development of nearshore bars: Aquitanian Coast, France. *Comptes Rendus Geosci* 338:795–801
- Ciavola P, Taborda R, Ferreira O, Dias JMA (1997) Field observations of sand-mixing depths on steep beaches. *Mar Geol* 141:147–156
- Ferreira O, Bairros M, Pereira H, Ciavola P, Dias JA (1998) Mixing depth levels and distribution on steep foreshores. *J Coast Res* 26:292–296
- Ferreira Ó, Ciavola P, Taborda R, Bairros M, Dias JMA (2000) Sediment mixing depth determination for steep and gentle foreshores. *J Coast Res* 16:830–839
- Fucella JE, Dolan RE (1996) Magnitude of subaerial beach disturbance during northeast storms. *J Coast Res* 12:420–429
- Greenwood B, Hale PB (1980) Depth of activity, sediment flux and morphological change in a barred nearshore environment. In: McCann SB (ed) The coastline of Canada. Geological Survey of Canada, Halifax, pp 89–109
- Ingle JC (1966) The movement of beach sand. Elsevier, New York
- King CAM (1951) Depth of disturbance of sand on sea beaches by waves. *J Sediment Petrol* 21(3):131–140
- Komar PD, Inman DL (1970) Longshore sand transport on beaches. *J Geophys Res* 75:5514–5527
- Kraus NC (1985) Field experiments on vertical mixing of sand in the surf zone. *J Sediment Petrol* 55:3–14
- Kraus NC, Isobe M, Igarashi H, Sasaki TO, Horikawa K (1982) Field experiments on longshore sand transport in the surfzone. In: Edge BL (ed) Proc 18th Coastal Engineering Conf, 14–19 November. Cape Town, ASCE, pp 970–988
- Lin P, Liu PLF (1998) A numerical study of breaking waves in the surf zone. *J Fluid Mech* 359:239–264
- Liu P, Dalrymple R (1978) Bottom frictional stresses and longshore currents due to waves with large angle of incidence. *J Mar Res* 36:357–375
- Masselink G, Short AD (1993) The effect of tide range on beach morphodynamics and morphology: a conceptual beach model. *J Coast Res* 9(3):785–800
- Nicholls RJ, Orlando SP (1993) A new dataset on the depth of disturbance and vertical erosion on beaches during storms. In: Bruun P (ed) Proc Int Coastal Symp, Hilton Head Island, SC, pp 230–235
- Saint-Cast F (2002) Modélisation de la morphodynamique des corps sableux en milieu littoral. PhD Thesis, University Bordeaux I
- Sherman DJ, Short AD, Takeda I (1993) Sediment mixing-depth and bedform migration in rip channels. *J Coast Res* SI 15:38–49
- Sunamura T, Kraus NC (1985) Prediction of average mixing depth of sediment in the surf zone. *Mar Geol* 62:1–12
- Van Rijn LC (1989) Handbook of sediment transport by currents and waves. WL Delft Hydraulics, The Netherlands, Report H461
- Walkden MJA, Hall JW (2005) A predictive mesoscale model of the erosion and profile development of soft rock shores. *Coast Eng* 52(6):535–563
- Williams AT (1971) An analysis of some factors involved in the depth of disturbance of beach sand by waves. *Mar Geol* 11:145–158